

RECYCLING NEUTRON STARS TO ULTRA SHORT PERIODS: A STATISTICAL ANALYSIS OF THEIR EVOLUTION IN THE $\mu - P$ PLANE.

Andrea Possenti¹, Monica Colpi², Ulrich Geppert³, Luciano Burderi⁴, Nichi D'Amico⁵

To Appear in ApJS

ABSTRACT

In this paper we investigate the statistical evolution of magnetic neutron stars, recycled in binary systems, simulating synthetic populations. To bracket uncertainties, we consider a soft (FP) and a stiff (PS) equation of state (EoS) for nuclear matter and explore the hypothesis that the magnetic field is confined in the stellar crust. We follow the magneto-rotational evolution within a simple recycling scenario. The decay of the magnetic field is modelled imposing at the crust–core boundary either complete field expulsion by the superconducting core or advection and freezing in a very highly conducting transition shell.

Irrespective to the details of the physical models we find the presence of a tail in the period distribution of the synthetic populations at periods shorter than 1.558 ms, the minimum detected so far. For the soft EoS, and independent of the details of the magnetic field evolution, the recycling gives rise to a spin distribution which is increasing monotonically toward short periods and a clear “barrier” forms at the minimum period for the onset of mass shedding ($\simeq 0.7$ ms). For the stiff EoS the distribution is flatter displaying a broad maximum about 2-4 ms. On the other hand, if in low mass binaries the neutron stars experience a progressive decrease of the mass accretion rate (due to transient behaviour and/or the quenching of accretion), the magnetospheric propeller produces (together with the magnetic dipole losses) an overall depletion of neutron stars in the millisecond region of the μ - P plane.

The estimated fraction of neutron stars spinning close to their shedding limit over the millisecond pulsar population is found to be significant. Crustal magnetic field decay models predict also the existence of massive rapidly spinning neutron stars with very low magnetic moment $\mu < 10^{25.8}$ G cm³.

¹Dipartimento di Astronomia dell'Universita', via Ranzani 1, 40127 Bologna, Italy

²Dipartimento di Fisica dell'Universita', via Celoria 16, 20133 Milano, Italy

³Astrophysikalisches Institut Potsdam, An der Sternwarte 16, 14482 Potsdam, Germany

⁴Osservatorio Astronomico di Monteporzio, via Frascati 33, 00044 Roma, Italy

⁵Osservatorio Astronomico di Bologna, via Ranzani 1, 40127 Bologna, Italy

Subject headings: magnetic field: general — equation of state — pulsars: general — stars: neutron

1. Introduction

PSR1937+21, at present, is the neutron star having the shortest rotational period $P_{min} = 1.558$ ms ever detected: It is a millisecond radio pulsar (MSP), the fastest among the ~ 30 discovered in the Galactic field with weak magnetic field and age $> 10^9$ yr. Despite its apparent smallness, P_{min} is not a critical period for NS rotation: NSs can indeed spin faster, as indicated by Cook, Shapiro & Teukolsky (1994). These authors showed that during recycling a bare non magnetic NS can attain periods as short as P_{min} with modest values of the rotational to potential energy ratio and modest values of the mass accreted ($< 0.1 M_{\odot}$), for all known equations of state (EoSs) of the nuclear matter. The period P_{min} is longer than the limiting period, P_{sh} , below which the star becomes unstable to mass shedding at its equator, irrespective to the EoS. It is clear that only the discovery of an ultra short period MSP (i.e. a weak field pulsar with P close to P_{sh}) would allow to set limits on the proposed EoSs; as an example, a very soft EoS permits pulsations at ~ 0.7 ms.

Burderi, Possenti, Colpi, Di Salvo & D’Amico (1999) noticed that the recycling of magnetic NSs to $P < 10$ ms depends sensitively on the mass transferred to the compact object and crucially on the evolution of the surface magnetic field. In particular, a slowly decaying magnetic field favours only the re-acceleration of a NS to $P \gtrsim 5 \div 10$ ms, while halving the request of mass accreted with respect to the case of a nonmagnetic star. Conversely, if a rapid and substantial decay of the surface magnetic field takes place, a NS can attain $P < P_{min}$. In this case, the minimum mass load necessary to approach P_{sh} is of $\sim 0.3 M_{\odot}$: it was calculated using the softest EoS (having $P_{sh} = 0.7$ ms) and introducing the most favourable *ad hoc* evolution for the decay of the magnetic field. In this paper we wish to study in details those processes which interfere positively to spin up a NS up to P_{sh} in a LMB. Among them, the most important are the evolution of the magnetic moment μ , and the evolution of the mass transfer.

At present, there is no satisfactory theory for the origin of the magnetic field and consequently several avenues of field decay are possible: The field can either be a fossil remnant from the progenitor star or be generated soon after the formation of the NS. Thus, an unanswered question is where the bulk of the magnetic energy is stored (Bhattacharya & Srinivasan 1991). If it resides mainly in the core (as in the case of a fossil field), the evolution of μ may be driven by variations in the rotational state of the NS, which affects the motion of the superfluid vortices and, in turn, of the fluxoids, carriers of the magnetic energy (Srinivasan *et. al* 1990; Ding, Chen & Cau 1993; Miri & Bhattacharya 1994; Ruderman 1998). If the magnetic energy is generated and confined in the thin crust of the NS (Blandford, Hernquist & Appelgate 1983; Urpin, Levshakov & Yakovlev 1986), the surface magnetic field decay is guided by the ohmic diffusion and the dissipation of electric currents (Sang & Chanmugam 1987: see § 3 for an updated set of references). The EoS valid for the core determines the thickness of the crust as well as the cooling history of the NS

which both affect strongly the magnetic field decay. In the case of a crust field however, magnetic evolution is not univocal, depending sensitively on the properties of the nuclear matter at the crust–core boundary, where superfluid (SF) and superconductive (SC) phase transitions may occur. As crustal matter is progressively assimilated into the core due to accretion, the magnetic field at the crust-core boundary can either be expelled (Urpin, Geppert & Konenkov 1998) or advected into the SC core where it no longer decays (Konar & Bhattacharya 1998). Thus, at the endpoint of evolution, the NS can either become non magnetic (on the long term), or preserve a relic field intense enough to shine again as MSP. These avenues are possible and the extent of the decay is intimately connected with the transfer rate and amount of matter accreted as heat released in the crust rises the electron and ion resistivity, accelerating the dissipation of current. Thus, field and mass transfer evolution couples intimately during the lifetime of the NS in a LMB.

Within the recycling scenario (Alpar et al. 1982; Bhattacharya 1995) all schemes suggested for the origin and the evolution of μ allow accreting NSs to reduce their magnetic moment to the values that are characteristic of MSPs (Urpin, Geppert & Konenkov 1998) but core models requires rather extreme conditions on the impurity content of crustal matter (Konar & Bhattacharya 1999). Only through a statistical approach it is possible to establish how efficient the recycling process is in spinning NSs to ultra short periods. This has been recognized first by Possenti, Colpi, D’Amico & Burderi (1998, paper I) who carried on a statistical analysis of NSs in the millisecond and submillisecond interval, using a population synthesis model. Their aim was to determine whether there might exist feasible conditions for spinning a significant number of NSs to $P < P_{min}$, during recycling in LMBs. They found first evidence of a tail in the distribution of MSPs at periods shorter than those detected so far. This possibility was met within empirical models that involve the screening by the accreting matter treated as a pure diamagnet (Bisnovatyi-Kogan & Komberg 1975), and models that call for a crustal nature of the magnetic field.

In this paper we modify the population synthesis calculation of paper I incorporating a detailed physical model for the evolution of a crustal magnetic field (using two boundary conditions to mimic expulsion or assimilation of the field by the SC core), adding further effects that might alter the statistical outcome. We also improve accuracy including the relativistic corrections (Burderi *et al.* 1999) necessary to describe the spinup process when the NS accretes matter from a disk, whose inner rim approaches the radius of the last quasi stable orbit.

The evolution in the μ - P plane is followed within a scenario of recycling, constructed using our knowledge of accretion in low mass X-ray binaries (LMXBs). The study is not aimed at correlating, on an evolutionary level, the observed population of LMXBs with the observed population of MSPs. MSPs may not be indeed the direct descendant of LMXBs: establishing this potential link or the link with LMBs forming through alternative evolutionary channels (Kalogera & Webbink 1996, 1998) would require the complete statistical knowledge of the orbital parameters, of the mass ratios, of the hydrodynamical processes guiding mass transfer and ultimately of the internal evolution and structure of the donor star (see e.g. Ergma, Sarna & Antipova 1998; Muslimov & Sarna 1993). These are aspects of a complex statistical calculation that is beyond our

purposes. We wish here to determine whether a minimal but possibly physically consistent model for the recycling can provide indications on the period distribution of NSs in the millisecond and sub-millisecond domain, as guide line for future searches. Our aim is also to address a number of questions that we are outlining below.

In our population synthesis model we account for the evolution during the early phases when the NS in the LMB behaves as if isolated and later when fed by wind accretion. The mass transfer during the Roche Lobe Overflow (RLO) phase is modelled just considering a range of accretion rates which is close to the one observed in LMXBs (Frank, King, & Raine 1992; Webbink, Rappaport & Savonije 1983). In a number of models, the accretion rate is treated as a constant over the RLO phase: This is an approximation as its actual behaviour follows a complex evolutionary pattern depending on the orbital parameters and on the degree of mass and orbital angular momentum losses (Ergma et al. 1998; Ergma & Sarna 1996).

The increasing evidence that NSs in LMXBs may suffer phases of transient accretion due to thermal viscous instabilities in irradiation dominated disk (e.g. van Paradijs 1996; King, Kolb & Szuszkiewicz 1997; King, Frank, Kolb & Ritter 1997) is suggestive that mass transfer onto a NS may not stop suddenly, at the end of the RLO: the star probably undergoes a progressive reduction of the mean accretion rate, modulated by alternate phases of higher and lower accretion. The effects of this transient behaviour on the evolution of the magnetic field is not known yet (Page, Colpi, Geppert & Possenti 1999, *in preparation*), but, if the magnetic field is not too weak, any drop in the accretion rate implies the growth of the typical dimension of the magnetosphere (Bhattacharya & van den Heuvel 1991, see § 2 for details). Dragged by the rapidly spinning NS, the magnetosphere can transform in a centrifugal barrier, accelerating the matter at the inner rim of the accretion disk on superkeplerian orbits (propeller effect: Illarionov & Sunyaev 1975); the extraction of angular momentum from the compact object that follows spins down the NS. *Does unsteady accretion at the end of the RLO phase vanish the effect of the previous phases of spinup? Is the potential population of very rapidly spinning NSs reflected back to $P > P_{min}$?* Many physical ingredients necessary to fully describe the propeller induced spindown are poorly known or difficult to assess (e.g. the exact law for the decrease of the mass transfer rate or the efficiency in the extraction of the angular momentum from the NS to the propelled matter). So, we studied the problem on a statistical basis, parametrizing the most uncertain quantities.

The fastest rotating NSs detected so far have been discovered at radio frequencies, and statistical analyses based on current samples of MSPs (Cordes & Chernoff 1997) have revealed that the pulsar distribution is increasing toward short periods with best-fit minimum period slightly below P_{min} . Radio Searches for very rapidly spinning objects are now in progress. In particular the large scale survey at the Northern Cross Radiotelescope near Medicina (D’Amico *et al.* 1998), has a sensitivity profile relatively flat in the submillisecond period range. If successful, these searches can potentially provide information on the EoS for nuclear matter (Burderi & D’Amico 1997; Phinney & Kulkarni 1994; Stergioulas & Friedman 1995). If NSs can be recycled up to P_{sh} , the observed population can retain features of the EoS. Yet, many factors influence the recycling

process, (magnetic moment evolution, total amount of mass disposable for the accretion, evolution of the mass transfer rate, propeller induced spin down and so on) likely spreading the observed distribution to slower spin rates and perhaps, in extreme cases, almost completely masking the effects of the EoS. Thus, *can we determine, on a statistical basis, whether recycled rapidly rotating pulsars preserve signatures, in their μ - P diagram, for a distinction between the EoSs?*

Both types of evolution for a magnetic field of crustal origin allow, to a different degree, for the decay of μ at values lower than those typical of the observed MSPs sample, and probably below the threshold for radio emission (Konar & Bhattacharya 1998; Geppert & Konenkov 1998; Sturrock 1971; Ruderman & Sutherland 1975). In view of these searches an additional question is worth exploring: *Can we find a distinct feature in the distribution of NSs reflecting the boundary conditions at the crust-core interface? How significant is the production of weakly magnetized NSs during recycling?* As with the previous case, the statistical approach will help in clarifying whether the behaviour of highly condensed matter can be inferred from a close analysis of the NS period distribution.

In the § 2 we outline the magneto-rotational evolution of a NS as predicted by the recycling scenario, introducing the parameters adopted for the calculation. In the § 3 we focus on the evolution of the magnetic field residing in the crust of an accreting NS, and describe the effects of different physical assumptions. In the § 4 we present the results of the population synthesis calculations, addressing one by one the questions risen in this § 1. § 5 contains the conclusions.

2. Spin Evolution Scenario

2.1. Physical model

According to the recycling scenario (e.g. Lipunov 1992), the NSs in low mass binaries (LMBs) may experience the phase of ejector, accretor, or propeller. In the ejector phase, the NS spins down only via radiation torque, and we assume dipole emission according to the simple law

$$\dot{P} = 3.15 \times 10^{-16} \frac{\mu_{26}^2}{P} \text{s yr}^{-1} \quad (1)$$

where P is the neutron star rotation period in seconds, μ_{26} is the magnetic moment in units of 10^{26} Gcm^3 .

In the propeller and accretor phases, matter penetrates down to the NS magnetosphere whose radius (Bhattacharya & van den Heuvel 1991) is

$$r_{mag} = 9.8 \times 10^5 \phi \mu_{26}^{4/7} \dot{m}^{-2/7} M^{-1/7} R_6^{-2/7} \text{ cm} \quad (2)$$

where ϕ is estimated following Burderi et al. (1998); in equation (2) M is the NS mass in solar masses, R_6 the static NS equatorial radius in units of 10^6 cm and \dot{m} the accretion rate in units of Eddington, i.e. $1.5 \times 10^{-8} R_6 M_\odot \text{ yr}^{-1}$. In the propeller state, the uniform angular velocity of

the NS is higher than the keplerian velocity at r_{mag} , and the magnetosphere acts as a centrifugal barrier (Illarionov & Sunyaev 1975). The infalling plasma is forced into super keplerian rotation and is propelled away: The NS loses angular momentum and spins down. The accretion phase sets in everytime the magnetosphere does not act as a barrier to matter approaching r_{mag} . In the statistical analysis of the RLO phase, we assume that the NS is fed through a disk whose inner radius r_{in} depends on the magnetic and rotational parameters of the NS. For high enough μ , the magnetic coupling between the disk and the star determines the extent of the angular momentum transfer: the corresponding value of r_{in} is r_{mag} . In general r_{mag} must be compared with both R_Ω and r_{ms} , where R_Ω is the physical equatorial radius of the NS (accounting for the inflation due to very fast rotation) and r_{ms} is the radius of the last stable orbit. If the magnetic field is very low ($\mu \lesssim 10^{26.5} \text{Gcm}^3$), r_{mag} is smaller than R_Ω (or r_{ms}) and the accretion disk is truncated directly at the NS surface ($r_{in} = R_\Omega$) or at the last stable orbit ($r_{in} = r_{ms}$).

The angular momentum balance relation used to follow the period evolution of the NS is

$$\frac{d(I_\Omega \Omega)}{dt} = g \dot{m} l_{in}, \quad (3)$$

where I_Ω is the moment of inertia of the rotating star, Ω its angular velocity and l_{in} the specific angular momentum of the accreting matter at the relevant inner radius r_{in} of the disk. The torque function $g = g(\Omega)$ accounts for the details of the angular momentum transfer between the NS magnetosphere and the accretion disk. When $r_{in} = r_{mag}$ and $g = 0.0$ the NS is on the so-called “spinup line”, where it can accrete mass without modifying its angular momentum $I_\Omega \Omega$. If the magnetospheric radius is inside the marginally stable radius r_{ms} or inside the star’s radius, we set $r_{in} = r_{ms}$ (or $= R_\Omega$), and g is equal to 1. When the NS is in a propeller state the function g becomes negative (see §2.2 for the values adopted). If the position of the NS in the $\mu - P$ plane at the end of mass transfer is above the “death line” (Sturrock 1971, Ruderman & Sutherland 1975), the NS shines as a *pulsar* and suffers secular spin down by magnetic dipole torques (eq. [1]). In this terminal phase, the pulsar migrates to the right of the $\mu - P$ diagram, drifting towards longer periods.

2.2. Values adopted for the synthesized populations

The NSs evolved in our population synthesis model have an initial gravitational mass of $1.4 M_\odot$. Cook, Shapiro & Teukolsky (1994) showed that all viable equations of state (EoSs) for nuclear matter allow for recycling a $1.4 M_\odot$ unmagnetized NS to ultra-rapid spinning rates. $P \lesssim 1.5$ ms are attained (before the mass-shedding instability disrupts the star) even in those models having a static maximum mass close to $1.4 M_\odot$. However, the minimum attainable period depends on the specific equation of state. We here investigated two EoSs: the FP-EoS (van Riper 1988) and the PS-EoS (Pandharipande & Smith 1975), similar to the A-EoS and the L-EoS of paper I (see Arnett & Bowers 1977 for the labelling of the EoSs). The FP is a soft equation of state (radius $R = 1.06 \times 10^6$ cm for a $1.4 M_\odot$ -static neutron star and central density

$\rho_c = 1.27 \times 10^{15} \text{ g cm}^{-3}$), whilst the PS is one of the stiffer ($R = 1.64 \times 10^6 \text{ cm}$ and $\rho_c = 3.6 \times 10^{14} \text{ g cm}^{-3}$ for the same canonical mass). In the most favourable circumstances and accreting $0.5 M_\odot$ (an acceptable amount for the baryonic mass transferred in a LMB), a NS can spin up to a period of $P_{sh} = 0.73 \text{ ms}$ (for FP-EoS) and of $P_{sh} = 1.40 \text{ msec}$ (for PS-EoS). These values have been computed according to Burderi *et al.* (1999), who developed a semi-analytical model for studying the evolution of the rotational period of a magnetic neutron star as a function of the accreted baryonic mass. The model permits the inclusion of general relativistic effects and comprises: (i) the stellar deformation (circumferential radius) as a function of angular velocity, (ii) the variation of the moment of inertia in response to the mass load and to the increasing rotation, (iii) the location of the marginally stable orbit for the computation of the angular momentum transfer rate in low-field NSs; (iv) the decrease of the mass shedding period for the compact object, due to the increase of the baryonic mass by accretion.

In our statistical model of paper I, we evolved NSs in low mass binaries (LMBs) through the five phases of the recycling scenario. Here, we start with a population of NSs at the onset of the Roche Lobe Overflow (RLO) phase. The adopted parameters are shown in Table 1. Urpin, Geppert & Konenkov (1998) calculated the tracks in the $\mu - P$ plane for a sample of pulsars, assuming different hypotheses for the binary evolution times, for the magnetic field decay and for the angular momentum transfer between the intervening plasma and the magnetosphere. Starting with pulsar parameters (μ_{ini} and P_{ini}) in accordance with the most updated observational analyses (Bhattacharya *et al.* 1992, Lorimer 1994, Hartman *et al.* 1997), they showed that, at the end of the wind phase, the typical NS magnetic field is about 1.5 – 3 orders of magnitude lower than at the onset of the pulsar phase (almost depending on the duration of wind accretion; see section §3), whilst the period P spreads between $\sim 0.1 \text{ sec}$ and $\sim 1000 \text{ sec}$. During the RLO accretion the spinup line is reached after a time $\tau_{sp} \simeq 10^5 \div 10^6 \text{ yr}$ which is shorter than the duration of the RLO accretion phase. Thus, the rotational evolution of a NS is almost independent of P at the onset of the RLO phase. Therefore, we adopted a simple flat distribution in period (see Table 1) as input parameter for the calculations, verifying that the statistical outcome of the subsequent phases are insensitive to the exact range of P or/and to its detailed initial distribution.

The logarithm of the accretion rate \dot{m} (in Eddington mass \dot{M}_E) during the RLO stationary phase is randomly selected from a gaussian distribution, with peak value ($0.1 \dot{M}_E$) and spread σ (half dex) compatible with the observed values. In fact, the typical X-ray luminosities of the stationary LMXBs cluster in the interval $10^{36} \rightarrow 10^{38} \text{ erg/sec}$ (van Paradijs 1995), implying accretion rate in the range $\sim 10^{-10} \rightarrow \sim 10^{-8} M_\odot/\text{yr}$ (for masses $\sim 1.4 M_\odot$). Uncertainties in distance of the sources and/or in the radiative efficiency of the accretion process could affect these estimates. We note that the typical mean accretion rates selected span the interval of values calculated by Ergma *et al.* (1998) within scenarios with conservative mass transfer. Low luminosity LMXBs may exist, yet undetected, so we explore lower mean rates on the synthesized population of recycled NSs.

As shown in Burderi *et al.* (1999), the minimum mass for spinning a *magnetized* $\sim 1.40 M_\odot$

NS up to $P < 10$ msec is $\sim 0.01 M_{\odot}$, (this value doubles for unmagnetized neutron stars). We adopt that value as lower limit to the total mass accreted, in our synthesized populations. As regard to the upper limit, the maximum value of the mass transferred (i) must grant for the radial stability of the accreting NS and (ii) has to be compatible with the maximum duration of the RLO phase τ_{RLO}^{max} . For both EoSs, the first criterion is safely satisfied by assuming an upper limit of $0.5 M_{\odot}$ (as extrapolated from Cook, Shapiro & Teukolsky 1994). The second request introduces a free parameter.

We considered a flat probability distribution for the logarithm of time of duration of the terminal phase of recycling, when the NS could emit as a radio. The minimum adopted value largely accounts for the time necessary to clean up the NS surroundings before the magnetic dipole emission could set in again. The maximum time is limited by the age of the disk of the galaxy, for which we put an upper limit on the total duration of the entire recycling process. The value of τ_{RLO}^{max} could be shortened if evaporation of the companion sets in (Muslimov & Sarna 1993) and we explore accordingly values as short as $\sim 10^7$ yr.

The behaviour of the function g and the value at which it zeroes (dubbed as critical fastness parameter $\Omega_{s,crit}$) are still uncertain. Therefore we adopted two different forms for g , following the suggestions of Ghosh & Lamb (1991) and of Wang (1996 and reference therein). However, both calculations considered only the positive branch of the g -function, which governs the transfer of angular momentum from the disk to the NS. For a slowly rotating NS, their estimates for the torque efficiency are respectively $g(\Omega = 0) = 1.17$ for Wang, and $g(\Omega = 0) = 1.40$ for Ghosh & Lamb. The predicted values of $\Omega_{s,crit}$ cover a larger range due to the different approximations used in the calculation. However we noticed that our results do not change sensitively if $\Omega_{s,crit}$ varies in the interval $0.85 \div 1.00$ (in units of the Keplerian angular velocity at the inner rim of the accretion disk) compatible with the most updated estimates (but see Li & Wang 1999 for a different view).

The shapes of the g -function near $\Omega_{s,crit}$ have to be assumed cautiously. No fully consistent calculation of the torque function is available yet for the description of the propeller phase. In order to include this effect (especially at the end of the RLO phase), we extrapolated the known g functions to their negative branch, introducing a central symmetry with respect to their zero-point. This preserves continuity and derivability with the minimum number of further physical hypotheses. Different semi-qualitative approximations (e.g. Menou, Esin & Narayan 1998 adopted a linear relation between g and Ω) do not affect our statistical findings once $\Omega_{s,crit}$ is close to 1.00.

2.3. *Persistent and non-stationary accretion*

During the RLO stage, very extended phases of constant accretion rate are quite improbable. For example, Muslimov & Sarna (1996) and Ergma et al. (1998) showed how \dot{m} can vary in LMBs under different hypothesis for the evolution of the system (conservative or non conservative mass

transfer, orbital angular momentum losses, initial orbital period and/or secondary evolutionary stage). With the aim of exploring the effect of a decreasing \dot{m} on the population of fastly spinning objects, we compared two possibilities: persistent accretion for a time τ_{RLO} , or persistent accretion for a shorter time followed by a transient phase mimicking the quenching of the mass transfer. We modelled the switching off of the accretion as a power law decay for \dot{m} , investigating the effect of varying the two parameters: (i) the ratio \mathcal{F}_{que} between the duration of the quenching phase with respect to the total RLO phase and (ii) the index Γ_{que} of the power law. Adopted values for \mathcal{F}_{que} range from 0.0 \rightarrow 0.5 and for Γ_{que} from 1 ($\dot{m} \propto t^{-1}$) to 10 (representative of an almost sudden switch off). Probably the quenching of the accretion is not a smooth process, but develops through alternate phases of higher and lower mass transfer rate, transforming the NS in a transient source of X-rays. Due to the short timescales of outburst and recurrence (with respect to the duration of the whole quenching process), our crude model could describe satisfactorily also this more realistic situation. On the contrary, our model can not account for those cases in which the accretion rate initially decreases and later increases substantially (in tight systems as indicated in Ergma et al. 1998; for MSPs recycled in Intermediate Mass Binaries as recently suggested in Podsiadlowski & Rappaport 1999).

We account for the angular momentum losses by propeller, both for persistent and for non-stationary accretion during phase IV. An extended spin down phase is quite unlikely in the former case, because a steady accretion rate and a reduced magnetic moment imply a very small magnetosphere. On the contrary, if, at the end of the RLO phase, \dot{m} decreases, the magnetospheric arm can increase, allowing for an efficient transfer of angular momentum from the NS outside.

3. Magnetic field evolution in LMBs

3.1. Physical model

A basic assumption for the present investigation is the crustal origin of the neutron star magnetic field, i.e. it is created at the beginning of the NS's existence in its crustal layers. The onset of a thermomagnetic instability, which transforms heat into magnetic energy during the early phases, is an effective tool to produce strong fields in the crust of a NS (Urpin, Levshakov & Yakovlev, 1986; Wiebicke & Geppert, 1996). Although that instability is not yet completely understood, it is a plausible mechanism which does not depend on special assumptions and may account for the observed variety in the NS magnetic field strengths. Moreover, the assumption of a crustal magnetic field is in accordance with the general accepted evolutionary scenarios for isolated NSs (Urpin & Kononkov, 1997), NSs in low mass binaries (Urpin, Geppert & Kononkov, 1998), NSs in high mass binaries (Urpin, Kononkov & Geppert, 1998) and millisecond pulsars (Geppert & Kononkov, 1998).

Since, at the beginning of the RLO phase, the anisotropies of the conductivity σ can be safely

neglected, the evolution of the MF is governed by the induction equation

$$\frac{\partial \vec{B}}{\partial t} = -\frac{c^2}{4\pi} \nabla \times \left(\frac{1}{\sigma} \nabla \times \vec{B} \right) + \nabla \times (\vec{v} \times \vec{B}), \quad (4)$$

where \vec{v} is the flux velocity of the accreted matter through the crust. When considering only the evolution of an axisymmetric dipolar poloidal field the induction equation can be simplified by introducing the vector potential $\vec{A} = (0, 0, A_\varphi)$ and choosing $A_\varphi = s(r, t) \sin \theta / r$. With the spherical radius r and the polar angle θ , both the radial and meridional field components can be expressed in terms of the quantity $s(r, t)$,

$$B_r = \frac{2s}{r} \cos \theta, \quad B_\theta = -\frac{\sin \theta}{r} \frac{\partial s}{\partial r}, \quad (5)$$

which gives the maximum field strength at the NS surface ($r = R$) by its polar value for B_r , that is $B_s(t) = 2s(R, t)/R$. Although in the outer layers of the crust the inflow of matter channeled by the magnetic field is certainly not radial, the mass flow will become nearly spherical symmetric in the higher density regions, where the currents are concentrated. In the approximation of a purely radial mass flow, $\vec{v} = -v_r \vec{e}_r$, the induction equation can be transformed to

$$\frac{\partial s}{\partial t} = \frac{c^2}{4\pi\sigma} \left(\frac{\partial^2 s}{\partial r^2} - \frac{2s}{r^2} \right) - v_r \frac{\partial s}{\partial r}, \quad (6)$$

where the flow velocity is given by the equation of continuity as

$$v_r = \frac{\dot{M}}{4\pi r^2 \rho}. \quad (7)$$

and $\dot{M} = \dot{m} \dot{M}_E$. While at the surface the standard boundary condition for a dipolar field applies, i.e. $R \partial s / \partial r + s = 0$, the inner boundary condition is more complicated and still a subject of scientific debates. In order to consider the possible different evolution of the NS magnetic field at the crust–core boundary we will apply two qualitatively different inner boundary conditions. During the accretion process onto a NS its field both diffuses and is advected towards inner layers. It is generally accepted that the core of a NS older than 10^9 yr is in a superfluid/superconductive (SF/SC) state, a state which will not be changed even by the intense heating during the RLO phase. Thus, in case of $\vec{v} = 0$, at the crust–core boundary the correct boundary condition is $s = 0$, since the Meissner–Ochsenfeld effect prevents the magnetic field from diffusion into the core. However, in case of $\vec{v} \neq 0$, the field, frozen in on timescales of matter flow, can cross the crust–core boundary and becomes assimilated in the core, together with the former crustal material. Our first boundary condition (BC I) assumes that, during the process of assimilation, \vec{B} will be expelled immediately by the crustal material undergoing the SF/SC phase transition. Thus we define:

$$\text{BC I :} \quad s = 0 \quad \text{at} \quad r = r_{\text{crust-core}}. \quad (8)$$

Alternatively we consider a second boundary condition (BC II), which allows an advection of the magnetic field into the core. There, it will be not further decayed due to SC but further advected

as long as accretion lasts. This assumption results in:

$$\text{BC II : } \quad s = 0 \quad \text{at} \quad r = 0 \quad . \quad (9)$$

which may cause the occurrence of a residual field remaining constant with time, (*freezing* of the field) whereas BC I allows for an exponential magnetic field decay down to zero. The situation assuming BC II has been described by Konar & Bhattacharya (1997) and we apply also their trick to simulate an effectively infinite conductivity in the assimilated core region.

For the density profile we assume that it will not be changed by the accretion of matter onto the NS. That is certainly a good approximation as long as no more than $\sim 0.1 M_{\odot}$ has been accreted. The chemical composition and density stratification can instead vary with increasing mass load ($0.1M_{\odot} \rightarrow 0.5M_{\odot}$) but these changes are considered unimportant, given the other approximations introduced.

At the beginning of the RLO, the currents maintaining the magnetic field are already located close to the crust–core boundary ($\rho_{\text{crust-core}} = 2 \times 10^{14} \text{ gcm}^{-3}$). Since even in the case of Eddington accretion the crust will not be heated up above $5 \times 10^8 \text{ K}$, the crustal matter at densities larger than 10^{10} gcm^{-3} is crystallized. Therefore, the relevant contributions to the electric conductivity in the crust are due to electron–phonon and electron–impurity scattering. Electron–phonon interactions dominates the transport at high temperatures and relatively low densities, whereas the impurity concentration determines the conductivity at lower temperatures and larger densities. The accretion induced heating of the crust diminishes the electron–phonon conductivity considerably since it is $\propto T^{-1}$ above the Debye temperature and $\propto T^{-2}$ for lower T . Fujimoto *et al.* (1984), Miralda–Escude *et al.* (1990) and Zdunik *et al.* (1992) calculated the crustal temperature as a function of the accretion rate. For both the stiff and the soft NS model, we used the following fitting formula, which gives the dependence of the crustal temperature T on the accretion rate in agreement with the numerical results of the above authors (see Urpin & Geppert, 1996):

$$\log T = 7.887 + 0.528 \left[1 - e^{-0.899(q+11)} \right], \quad (10)$$

where $q = \log(\dot{M}/M_{\odot} \text{ yr}^{-1})$. For $\log(\dot{M}/M_{\odot} \text{ yr}^{-1}) > -9.5$, Eq. [10] yields probably a somewhat too small crustal temperature. We use the numerical data for the phonon conductivity σ_{ph} obtained by Itoh *et al.* (1993) and a simple analytical expression for the impurity conductivity σ_{imp} derived by Yakovlev & Urpin (1980). The total conductivity is given by

$$\frac{1}{\sigma_{tot}} = \frac{1}{\sigma_{ph}} + \frac{1}{\sigma_{imp}} . \quad (11)$$

The lowest accretion rate we will consider for the RLO phase is $\log(\dot{M}/M_{\odot} \text{ yr}^{-1}) = -11$, which corresponds to a crustal temperature of about $8 \times 10^7 \text{ K}$. For such and higher temperatures, σ_{ph} is the dominating contribution to the conductivity in the whole crust. Besides on the temperature, density and impurity concentration, the conductivity depends on the chemical composition of the crust too. During an extended RLO phase the whole mass of the crust can be replaced by accreted

matter. Therefore, instead to assume that the crust is composed of cold catalyzed matter we apply the chemical composition established by the pycnonuclear reactions in the course of the accretion (see Haensel & Zdunik, 1990). The electric conductivities for the weakest and the strongest RLO accretion rates considered in this paper are shown in Fig. 1.

The density profile for the soft–EoS NS is given by van Riper 1988 (see Fig. 1 in Geppert & Urpin 1994), whereas the density profile for the stiff–EoS NS is taken from Pandharipande & Smith (1975). The EoS valid in the core determines the thickness of the crust and hence the scale of the crustal field. Hence, apart from the accretion driven decay mechanisms, it governs strongly the field evolution: the softer the EoS the faster the crustal field decays. This correlation is partly counterbalanced by relativistic effects which become stronger the softer the EoS is (Sengupta 1998).

In Figure 2 we represent (for $5 \times 10^6 \leq \tau_{RLO} \leq 5 \times 10^8$ yr) the decay of the surface magnetic field under the influence of different accretion rates during the RLO phase both for soft and stiff EoS and for the two boundary conditions considered here. The BC I allows for an exponential decay down to zero if the accretion period is extended enough. It is clearly seen that the larger the accretion rate the hotter the crust (see eq. [10]) and, hence, the more rapid the crustal field decays. The more rapid decay in case of the soft EoS in comparison with the stiff one is a result of the smaller spatial scale of the magnetic field. For both EoS we see that the assumption of BC II results in a much stronger surface field. Only for nearly Eddington accretion rates and soft EoS (lower right panel: curve labelled by -8.5), the very rapid field decay is practically unaffected by the choice of the boundary condition. In that case, perhaps, effects of submergence play an important role because for such large accretion rates the characteristic time for the mass flow in the lower density layers of the crust is smaller than the ohmic (re-)diffusion time in that region. For the soft EoS a trend in establishing a residual field is at most suggested for $\log(\dot{M}/M_{\odot} \text{ yr}^{-1}) = -10$ and -9.5 . The existence of residual fields seems to be much more evident for stiff EoS. For the lowest accretion rates the velocity of mass flow at the crust–core boundary is certainly too small to create residual fields during $\tau_{RLO} \leq 5 \times 10^8 \text{ yr}$ and for the near Eddington accretion the effect of submergence acts. However, for $\log(\dot{M}/M_{\odot} \text{ yr}^{-1}) = -9, -9.5$ and -10 , the development of a residual *frozen* field is clearly seen and its strength is positively correlated to the accretion rate, as Konar & Bhattacharya (1998) recently pointed out.

3.2. Values adopted for the synthesized populations

The typical value of the magnetic moment μ for the observed pulsar population lies in the range of $10^{29.5} \div 10^{31.5} \text{ Gcm}^3$ (Bhattacharya *et al.* 1992, Lorimer 1994, Hartman *et al.* 1997). During the subsequent evolutionary stages in a LMB, μ decays either by ohmic diffusion during the cooling of the NS (ejector and/or propeller phase) or by accretion driven decay mechanisms during the comparatively extended wind accretion phase, which can last up to 10^{10} years. In these phases the depth of the crust initially penetrated by the magnetic field determines its strength.

When the standard NS enters the RLO phase it has an age $\gtrsim 10^9$ yrs, and the field have had enough time to diffuse down to the crust–core boundary, where the steep increase of the electric conductivity prevents further inward diffusion, wherever the field was initially contained. Thus, at the onset of RLO, the field is located at the core-crust boundary, and its absolute strength is the parameter to be varied in the population synthesis. Examining the various paths in the $\mu - P$ plane calculated either by Geppert & Konenkov (1998), or by Urpin, Geppert & Konenkov (1998), it appears that, at the end of the wind phase, the bulk of the evolved NSs group on the μ -axis at values around $10^{28} \div 10^{29.5}$ Gcm³. Such a clustering of the NSs, in a relatively narrow interval in μ , allows us to bar the uncertainties in the magnetic evolution of the objects during the first three stages of the recycling scenario. The values μ_0 for the magnetic moment at the onset of the RLO era (t_0^{RLO}) are selected from a gaussian distribution (see Table 1) with a mean chosen in that interval.

4. Results & Discussion

To execute the evolution we built a Monte Carlo code, typically using 3,000 particles. The statistical analysis is performed only on those NSs reaching the so-called “millisecond strip” at the end of the fifth stage (*radio*) of the recycling scenario, the ones having period $P \leq 10.0$ ms and whichever value of the magnetic moment μ . In accordance with the values of P_{min} and μ_{min} (the weakest magnetic moment observed in PSRJ2317+1439; $\mu_{min} = 7.3 \times 10^{25}$ G cm³), we divided our particles in four groups. Those filling the first quadrant in the millisecond strip ($P \geq P_{min}$ and $\mu \geq \mu_{min}$) behave as the known MSPs. Also the objects belonging to the second quadrant ($P < P_{min}$ and $\mu \geq \mu_{min}$) should shines as pulsars (see Burderi & D’Amico 1997 and the discussion of § 1). The effective observability of the objects in the third quadrant ($P < P_{min}$ and $\mu < \mu_{min}$) as radio sources represents instead a challenge for the modern pulsar surveys. Most of them will be above the Chen and Ruderman (1993) “death-line”, and might have a bolometric luminosity comparable to that of the known MSPs. Thereafter we shortly refer as *sub-MSPs* to all the objects having $P < P_{min}$ and μ above the “death-line”. Objects in the fourth quadrant ($P \geq P_{min}$ and $\mu < \mu_{min}$) are probably radio quiet neutron stars (RQNSs), because they tend to be closer to the theoretical “death-line”, and they are in a period range which was already searched with good sensitivity by the radio surveys.

4.1. Are submillisecond pulsars a natural outcome of evolution in LMBs?

In this paragraph, we discuss the results of our population synthesis calculations with no inclusion of the propeller effect. We will refer thereafter as *standard* models. In Fig. 3, we report the observed sample of MSPs and the calculated populations for the two EoSs and the two adopted boundary conditions at the crust-core interface. The input parameters are those of Table 1 with $\tau_{RLO}^{max} = 5 \times 10^8$ yr. It appears that objects with periods $P < P_{min}$ are present in a statistically

significant number. In effect, though the detailed distributions of particles in the millisecond strip are influenced either by the EoS and by the magnetic field decay (see also Figs. 4 & 5), *a tail of potential sub-MSPs always emerges.*

In the synthetic sample for the *soft*-EoS, the “barrier” at $P_{sh} \simeq 0.7$ ms is clearly visible in Fig. 3, indicating that the field decay in longlived persistent LMBs proceeds fast enough to allow a significant fraction of objects to attain P_{sh} . The results are more clearly illustrated in Fig. 4 (solid line): the *soft-EoS gives rise to period-distributions that increase rather steeply toward values smaller than 2 ms*, irrespective to the adopted BCs. Instead, the boundary condition affects the distribution on μ : BC II produces a smaller number of objects with low field, as the field initially decays but, when the currents are advected toward the crust-core boundary, their decay is halted and the field reaches a bottom value. In particular, as already found in paper I where a BC of type II was considered, the fourth quadrant in Fig. 5 is underpopulated (see also Tab. 2).

The very *stiff*-EoS permits periods P longer than 1.4 ms, but the minimum observed period P_{min} is already close to the “barrier” of mass shedding. Moreover, the field decay establishes on time scales longer than for a soft EoS and, on average, the sample of objects has a higher mean field. As a consequence, only fewer objects appear on the left of P_{min} (Fig. 3). NSs with $\mu < \mu_{min}$ are rare objects for a BC of type II, and the ratios of *sub*-MSPs to MSPs are reduced with respect to the soft EoS (for the boundary condition BC II we have 0.003 for the stiff EoS and 0.573 for the soft one; see Table 2 for a complete review of the results).

Major differences appear also examining Fig. 4 (solid line): The period distribution for the stiff-EoS is much flatter than that for the soft-EoS, displaying a broad maximum at $P \sim 3$ ms. It was recently claimed that X-ray sources in LMBs (possible progenitors of the MSPs, see § 4.4 for details) show rotational periods clustering in the interval $2 \rightarrow 4$ ms (White & Zhang 1997; van der Kluis 1998). This effect could be explained introducing a fine tuned relation between μ and \dot{m} ($\mu \propto \dot{m}^{1/2}$: White & Zhang 1997). Alternatively, gravitational waves emission has been invoked: either due to the growing of *r*-mode instability in the accreting NS (Andersson, Kokkotas & Stergioulas 1998) or due to a thermally induced quadrupole moment in the NS crust (Bildsten 1998). Here we note that such a clustering can be a natural statistical outcome of the recycling process.

4.2. *Is unsteady or transient accretion in LMBs a threat to the existence of sub-MSPs?*

The suggestion that NSs in low mass binaries may become transiently accreting sources after having experienced a phase of persistent accretion prompted us to consider the effect of decreasing the mean accretion rate \dot{m} to mimic either the quenching of the accretion phase or the phases of quiescence in transient sources. If the magnetic field is high enough for the magnetosphere to affect the flow, the propelled matter may transfer outward the angular momentum of the NS. Therefore, we have considered the possibility that the NSs spend a fraction of the RLO phase

in transit to final quiescence. The quenching of the accretion rate was modelled with a simple power law in time with index Γ_{que} lasting a fraction \mathcal{F}_{que} of the duration of the RLO phase. The Figures 4, 6, 7 & 8 and the Table 2 show a summary of the results.

In Fig. 4 the dashed areas give the distributions of the NSs at the end of evolution, including a strong propeller phase ($\mathcal{F}_{que} = 0.50; \Gamma_{que} = 8$) during the quenching of the RLO. The emerging distributions are depleted of the fastest rotating NSs. However, it is remarkable that *for the soft EoS the distributions preserve a maximum just about P_{min} .*

In Fig. 6 we display the distribution on P of our synthesized populations at the end of the RLO phase (including strong propeller: dashed lines) and at the end of the magnetic dipole emission phase (dashed areas). It appears that dipole losses produce a clear shift of the entire population toward longer periods. However, it affects preferentially the distribution of NSs at periods longer than ~ 4 ms. In our simulation we have noticed that dipole losses reduce considerably the number of NSs in the millisecond strip (especially for $\mu > \mu_{min}$). In particular Fig. 7 shows that dipole losses are much more effective than a mild propeller ($\mathcal{F}_{que} = 0.25; \Gamma_{que} = 1$) in drifting the overall population at $P > 10$ ms, whereas it only slightly influences the very rapidly spinning objects.

Figure 7 allows also for the comparison of the different number of objects synthesized in the millisecond strip with different models. These numbers mainly depend on the timescale for μ to decay down to $\sim 10^{27.5}$ Gcm³, the value requested for a particle to enter the millisecond strip: the shorter the decay timescale is, the more filled is the millisecond strip. With BC I, the soft EoS gives a number of objects that is about 50% greater than the stiff EoS. For BC II such a distinction is smoothed except for a very short RLO phase ($\tau_{RLO}^{max} \simeq 5 \times 10^7$ yr), for which the freezing of μ is not operating yet.

Comparing Fig. 8 with Fig. 5, we note that *a strong propeller can threaten the formation of NSs with $P < P_{min}$ and $\mu > \mu_{min}$* especially in the case of the stiff-EoS (see Tab. 2). For objects with $\mu < \mu_{min}$, the spin-down torque is weaker: accordingly, the III quadrant is less depleted than the second one and a non number of low magnetic field fastly spinning NSs can survive at periods $\simeq 1$ ms, for the soft EoS.

Our statistical analysis can provide also information on the NS mass distribution as a function of P at the end of evolution (Fig. 9). We find that the mass function steepens toward high values when P falls below P_{min} : the distribution approaches values close to $M \sim 1.7 \div 1.8M_{\odot}$ as a large mass deposition is required to spin a NS to ultra short periods (we defer to Burderi *et al.* 1999 for a discussion on the minimum mass of NSs close to P_{sh}). LMBs could harbour NSs with such high values of the mass and a first indication comes from Casares, Charles & Kuulkers (1998) who inferred for Cyg X-2 a lower mass limit of $1.88 M_{\odot}$. The action of the propeller during evolution has the clear effect of inhibiting the mass infall: the mass distribution is only slightly affected for the soft EoS, while for the stiff EoS the difference is more pronounced.

4.3. A tool for discriminating EoS and μ -decay ?

In this paragraph we summarize the results of our statistical analysis considering in particular those objects having $P < P_{min}$. Table 2 collects the main results derived for the different scenarios (indicated in column ten). *Standard* evolution is that discussed in § 4.1. The other cases comprise a *propeller* phase at the end of the RLO (§ 4.2): here we adopted a propeller of intermediate effectiveness ($\mathcal{F}_{que} = 0.25$ and $\Gamma_{que} = 1$). To account for the uncertainties in the distribution of the accretion rates and/or in the maximum duration of the RLO stage, we run synthesis calculations either in the case of a *low* \dot{m} ($\dot{m} = 0.01 \text{ M}_{\oplus}$) or in the case of a *short* RLO phase ($\tau_{RLO}^{max} = 5 \times 10^7$ yr). Finally we combined the last two hypotheses.

The results are grouped by columns according to the adopted BC and by rows as regard to the EoS. In particular, columns 2 (for BC I) and 6 (for BC II) give the number of MSPs produced during the runs, normalized to the number of MSPs (set equal to 1000) synthesized in the case labelled by (iii) in the eleventh column. These figures give an estimate of the efficiency of the recycling process in producing objects in the first quadrant. The third (for BC I) and the seventh columns (BC II) give the fraction of NSs in quadrant II relative to I. The fourth and the eighth columns (respectively for BC I and BC II) report the fraction (II+III)/I while in brackets we give f_{sub} , i.e., the fraction of NSs with $P < P_{min}$ and μ lying above the death line relative to the sample of NSs filling quadrant I.

The estimate of f_{sub} can give indication on the fraction of *sub*-MSPs relative to the observed MSPs: if selection criteria similar to those found in the interval $P_{min} < P < 10.0$ ms apply as well at periods below P_{min} , f_{sub} provides an estimate of the number of pulsars that might be observable below P_{min} . We find that f_{sub} varies between 0% \rightarrow \sim 57%; the lower figure applies only to the case of an EoS of extreme stiffness: these objects should be observable with experiments like the survey in progress at the Northern Cross radio telescope near Medicina (D’Amico *et al.*,1998), which has similar sensitivity in the MSPs and in the *sub*-MSPs range.

Inspection of the Table 2 suggests that the EoS for the nuclear matter has a major role in determining the ratio f_{sub} : the formation of a *sub*-MSP is quite a rare event, for the very stiff EoS. On the contrary, in the case of a moderately soft EoS, the *sub*-MSP population is significant, irrespective to the details of the evolutionary scenario. Thus, the detection of a significant number of *sub*-MSPs would be strongly suggestive of a not too stiff EoS. A clear distinction in the models can be seen comparing case (iv) with (ix). If a moderate propeller takes place and the typical RLO timescale is shorter than usually assumed, for a soft-EoS $f_{sub} \simeq 30\%$ (irrespective the BC), whilst no *sub*-MSPs could appear if the nuclear matter behaves as predicted by the stiff-EoS. The details of the evolution can blend the outcome of the statistical analysis preventing a clear distinction between the equation of states when based on the simple ratio f_{sub} (e.g. cases (i), (ii) and (iii) versus (x) for the BC I). The boundary condition for the magnetic field at the crust-core interface weakly affects the figures of Table 2 (except for case (viii)) when considering only the objects filling the I and the II quadrant (compare the columns 2 and 3 with the columns 6 and 7).

Due to their effects on the decay of the surface magnetic field, *the differences between the two BCs are revealed mainly in the synthesized populations having $\mu < \mu_{min}$.*

4.4. Very low magnetic field NSs spinning at millisecond periods?

Except for the most unfavorable case (very stiff-EoS & BC II), all our synthesis runs produce a significant amount of objects with $\mu < \mu_{min}$ (see III & IV quadrants in the Figs. 5 & 8). Their period distribution is very sensitive to the adopted internal boundary condition for the magnetic field diffusion at the crust–core interface. BC II clearly favours fastly rotating objects ($P \lesssim 1.5$ ms), the IV quadrant in Figs. 5 & 8 being (scarcely) populated only in the case of a very strong propeller. For BC I the distributions are broader and the stiffer the EoS is the more depleted is the III quadrant. In principle, such a distinction could allow a discrimination among the two BCs.

On the observational point of view, very low magnetized NSs in the IV quadrant (upon which we focus in this paragraph) might be elusive sources. Irrespective to the selection effects or survey sensitivity thresholds, these objects might be rather close to the theoretical “death line” to be observable as radio, and it is not clear if we can observe them in the X-ray band.

Recently a neutron star rotating in the millisecond interval (SAX J1808.4-3658 with $P = 2.49$ ms) has been detected in X-rays (Wijnands & van der Kluis 1998). It is in a binary system with a low mass companion (Chakrabarty & Morgan 1998) which transfers mass to the compact object. As the rotational period is known, one can constrain the surface magnetic field of the accreting NS (Psaltis & Chakrabarty, 1998). An upper limit on μ relies on the requirement (a) that accretion is not centrifugally inhibited at the minimum accretion rate at which coherent pulsations are detected. The standard disk-magnetosphere model (Pringle & Rees 1972) interprets coherent X-ray pulsations as due to a complete or a partial funnelling of the disk plasma along the NS magnetic field lines. Many improvements had to be added to this model (Ghosh & Lamb 1991 for a review) to account for the variety of observations (e.g. Bildsten 1997); but in this framework, (b) a rotating NS can appear as an accretion powered pulsar only if the magnetic moment is strong enough to terminate the Keplerian disk above the stellar surface (Psaltis & Chakrabarty 1998; Burderi & King 1998). This requirement translates in a lower boundary on the possible value of μ . For the case of SAX J1808.4-3658, Psaltis & Chakrabarty (1998) found $3 \times 10^{25} \lesssim \mu \lesssim 10^{27}$ Gcm³, with a preferred value about a few times 10^{26} Gcm³. So, this object seems to be placed near the separation of the quadrants I and IV. Alternative models, not related or poorly related to μ , could explain coherent X-ray modulation at the NS spin frequency (e.g. azimuthal variation in optical depth for absorption or scattering) from which no further constraints on μ arise.

Already from the half of the nineties, the spin periods for a handful of NSs in low mass X-ray binaries have been inferred either from coherent pulsations during Type-I bursts or, indirectly, from the so-called kHz-QPOs (van der Kluis 1998 for a review). In the latter case, the paradigm is the so-called beat frequency model, in which the frequency difference $\Delta\nu_{qpo}$ among the two peaks

appearing in the X-ray power spectrum of the source is representative of the spin frequency of the NS or of an overtone (Miller, Lamb & Psaltis 1998). From the inferred spin, and assuming that these NSs rotate at about their equilibrium period (that is, near their competing spinup line), one can estimate (through condition (a)) the value of μ . As a representation, in Fig. 3, we display (*open squares*) the positions of the NSs of this group in the $\mu - P$ plane, adopting the values of White & Zhang (1997 and reference therein for a discussion about the errors in the determination of P and μ). It appears that no X-ray source shows $\mu < \mu_{min}$.

Prompted by the evidence of a not constant value for $\Delta\nu_{qpo}$ (Psaltis *et al.* 1998; Mendez & van der Klis 1999), other models for explaining the kHz-QPOs have been proposed. For instance, Stella & Vietri (1999) interpret the upper QPO frequency ν_2 as due to matter inhomogeneities orbiting the NS at the inner disk boundary (just as in the standard beat frequency model), whilst the lower QPO frequency ν_1 is produced by the periastron precession at the inner edge of the accretion disk. Apart from negligible corrections (due to the effect of the NS rotation on the exterior metric), the observed difference $\Delta\nu_{qpo} = \nu_2 - \nu_1$ is unrelated to the spin frequency of the NS. Being P not constrained by the observation, condition (b) for a lower limit on μ does not apply anymore. Hence we argue that also the magnetic moment estimates become questionable in this framework. As a consequence, some of the sources shown in Fig. 3 could be misplaced in the $\mu - P$ plane and, when accretion will halt, they could eventually enter the category of low magnetic field NSs. A similar suggestion was raised by Lai (1998), who constructed refined slim disk models in LMBs, incorporating the effects of both magnetic field and general relativity: for the kHz-QPO sources he found values of the surface magnetic field smaller than the previous authors. If this is the case, the values of μ in kHz-QPO sources ($\lesssim 10^{25}$ Gcm³) are systematically weaker than those of MSPs sample and these X-ray emitting objects would populate our IV quadrant.

As a general comments on the observability of low magnetic field NSs in the X-ray band, we note that if the capability of coherently emitting X-rays pulses requires high enough values of μ , missing rotating NSs with P close to a millisecond would not be surprising: as already shown in Burderi *et al.* (1999) and here confirmed, only a rapid and substantial decay of μ allows a NS to reach $P < P_{min}$. Therefore, low magnetic field fastly spinning NSs could be just those not showing coherent X-ray pulsations. Instead, the signature of very rapidly spinning objects might hopefully emerge from low amplitude features in their power spectrum, related to not coherent modulation of the X-ray brightness.

5. Conclusions

The population synthesis calculation has shown that:

1. Detailed models for the decay of the crustal magnetic field, including also refined relativistic corrections, show the presence of a tail in the period distribution of the synthetic NSs population at periods shorter than 1.558 ms.

2. For the soft EoS, and irrespective to the boundary condition at the crust-core interface for the magnetic field evolution, recycling in LMBs gives rise to a NS distribution which is increasing towards shorter periods, and a clear barrier is present at the minimum period for mass-shedding. For the stiff EoS, the distribution is flatter.
3. If NSs at the end of the persistent accretion in a LMB experience a phase of smooth decrease of the accretion rate (to mimic transient sources and/or quenching of accretion), the magnetospheric propeller produces a depletion of fastly spinning NSs but, at least for the soft EoS, it preserves a distribution that peaks at periods ~ 1.5 ms.
4. The estimated fraction of *sub*-MSPs over the entire MSPs population varies between 0 to $\simeq 50\%$. The adopted EoS and the parameters for the recycling play an important role in determining those percentages. The detection of such rapid rotating compact objects represents a challenge for the modern searches.
5. The models for the decay of a crustal magnetic field predict the existence of spun up NSs with very low magnetic moment: their period distribution is a neat signature for the physics at the crust–core interface.

The first two authors want to acknowledge the hospitality of the members of the *Astrophysikalisches Institut Potsdam* during the early phase of this work.

REFERENCES

- Alpar, M.A., Cheng, A.F., Ruderman, M.A., & Shaham, J. 1982, *Nature*, 300, 728
- Andersson, N., Kokkotas, K.D., & Stergioulas, N. 1998, astro-ph/9806089
- Arnett, W.D., & Bowers, R.L. 1977, *ApJS*, 33, 415
- Bhattacharya, D. 1995, in *X-ray Binaries*, ed. W.H.G. Lewin, J. van Paradijs & E.P.J. van den Heuvel (Cambridge Univ. Press), 5
- Bhattacharya, D. & van den Heuvel, E.P.J. 1991, *Phys.Rep.*, 203, 1
- Bhattacharya, D., Wijers, R., Hartman, J., Verbunt, F. 1992, *A&A*, 254, 198
- Bildsten, L. 1997, *ApJS*, 113, 367
- Bildsten, L. 1998, *ApJ*, 501, L89
- Bisnovatyi-Kogan, G.S. & Komberg, B.V. 1975, *SvA*, 18, 217
- Burderi, L., Di Salvo, T., Robba, N.R., Del Sordo, S., Santangelo, A., Segreto, A., 1998, *ApJ*, 498, 831
- Burderi, L., & D’Amico, N. 1997, *ApJ*, 490, 343
- Burderi, L., & King, A.R. 1998, *ApJ*, 505, L135
- Burderi, L., Possenti, A., Colpi, M., Di Salvo, T., D’Amico, N. 1999, *ApJ*, 519, 1 July
- Casares, J., Charles, P., & Kuulkers, E. 1998, *ApJL*, 493, L39
- Chakrabarty, D., & Morgan, E.H. 1998, *Nature*, 394, 345
- Chen, K. & Ruderman, M. 1993, *ApJ*, 402, 264
- Cook, G.B., Shapiro S.L., & Teukolsky, S.A. 1994, *ApJL*, 423, L117
- Cordes, J.M. & Chernoff, D.F. 1997, *ApJ*, 482, 971
- D’Amico, N., et al., 1998, *Proc. Symp. Neutron Stars and Pulsars*, Tokyo, Japan, 235
- Ding, K.J., Chen, K.S., & Chau, H.F. 1993, *ApJ*, 408, 167
- Ergma, E., Sarna, M.J. & Antipova, J. 1998, *MNRAS*, 300, 352
- Ergma, E., & Sarna, M.J. 1996, *MNRAS*, 280, 1000
- Frank, J., King, A.R., & Raine, D. 1992, *Accretion Power in Astrophysics*, Cambridge University Press

- Fujimoto, M., Hanava, T., Icko Iben, Jr., Richardson, M. 1984, ApJ, 278, 813
- Geppert, U., & Urpin, V. 1994, MNRAS, 271, 490
- Geppert, U., & Konenkov, D., 1998, Proc. of Symp. “Neutron Stars and Pulsars”, Tokyo, Ed. N. Shibazaki, N. Kawai, S. Shibata, T. Kifune, Universal Academy Press, Inc.,
- Ghosh, P., & Lamb, F.K. 1991, Neutron Stars: Theory and Observations, Kluwer, 363
- Haensel, P., & Zdunik, J.L. 1990, A&A, 227, 431
- Hartman, J.W., Verbunt, F., Bhattacharya, D., Wijers, R.A.M.J. 1997, A&A, 322, 477
- Illarionov, A., & Sunyaev R. 1975, A&A, 39, 185
- Itoh, N., Hayashi, H., & Kohyama, Y. 1993, ApJ, 418, 405
- Kalogera, W., & Webbink, R.F. 1996, ApJ, 458, 301
- Kalogera, W., & Webbink, R.F. 1998, ApJ, 493, 351
- King, A.R., Frank, J., Kolb, U., Ritter, H. 1997, ApJ, 484, 844
- King, A.R., Kolb, U., & Szuszkiewicz, E. 1997, ApJ, 488, 89
- Konar, S., & Bhattacharya, D., 1997, MNRAS, 284, 311
- Konar, S., & Bhattacharya, D., 1998, astro-ph/9808119
- Konar, S., & Bhattacharya, D., 1998, astro-ph/9812035
- Li, X.D., & Wang, Z.R. 1999, astro-ph/9901083,
- Lipunov, V.M. 1992, *Astrophysics of neutron stars*, Springer, Berlin
- Lorimer, D.R. 1994, Ph.D. Thesis, University of Manchester, U.K.
- Menou, K., Esin, A.A., & Narayan, R. 1998, astro-ph/9810323
- Miller, M.C., Lamb, F.K., & Psaltis, D. 1998, ApJ, 508, 791
- Miralda-Escude, J., Haensel, P., & Paczynski, B. 1990, ApJ 362, 572
- Miri, M.J., & Bhattacharya, D. 1994, MNRAS, 269, 455
- Muslimov, A.G. & Sarna, M.J. 1993, MNRAS, 262, 164
- Pandharipande, V., & Smith, R. 1975, Nucl.Phys. A, 237, 507
- Phinney, E.S., & Kulkarni, S.R. 1994, Ann. Rew. Astron. & Astrophys.

- Podsiadlowski, Ph. & Rappaport, S. 1999, astro-ph/9906045
- Possenti, A., Colpi, M., D'Amico, N., Burderi, L. 1998, ApJL, 497, L97 (paper I)
- Psaltis, D., *et al.* 1998, ApJ, 501, L95
- Psaltis, D., & Chakrabarty, D. 1998, ApJ submitted, astro-ph/9809335
- Pringle, J.E. & Rees, M.J. 1972, A&A, 21, 1
- Ruderman, M.A. & Sutherland, P.G., 1975, ApJ, 196, 51
- Ruderman, M.A., Zhu, T., & Chen, K 1998, ApJ, 492, 267
- Sang, Y., & Chunmugam, G. 1987, ApJ, 323, L61
- Sengupta, S. 1998, ApJ, 501, 792
- Srinivasan, G., *et al.* 1990, Curr.Sci. 59, 31
- Stella, L., & Vietri, M. 1999, Phys. Rev. Lett. 82, 17
- Stergioulas, N., & Friedman, J. 1995, ApJ, 444, 306
- Sturrock, P.A. 1971, ApJ, 164, 529
- Urpin, V.A., & Geppert, U. 1996, MNRAS, 278, 471
- Urpin, V.A., Geppert U., & Konenkov, D. 1998, MNRAS, 295, 907
- Urpin, V.A., & Konenkov, D. 1997, MNRAS, 284, 741
- Urpin, V.A., Konenkov, D., & Geppert, U. 1998, MNRAS, 299, 73
- Urpin, V.A., Levshakov, S.A., & Yakovlev, D.G. 1986, MNRAS 219, 703
- van der Klijs, M. 1998, in *The Many Faces of Neutron Stars*, eds. Alpar, Buccheri, van Paradijs, Dordrecht: Kluwer, 337
- van Paradijs, J. 1995, in *X-Ray Binaries*, eds. Lewin, van Paradijs, van den Heuvel, Cambridge University Press
- van Paradijs, J. 1996, A&A, 464, L139
- van Riper, K.A. 1988. ApJ, 329, 339
- Yakovlev, D., & Urpin, V. 1980, SvA, 24, 303
- Wang, Y.-M., 1996, ApJL, 465, L111

Webbink, R.F., Rappaport, S.A., & Savonije, G.J. 1983, ApJ, 270, 678

White, N.E., & Zhang, W. 1997, ApJL, 490, L87

Wiebicke, H.J. & Geppert, U. 1996, A&A, 309, 203

Wijnands & van der Kluis, M. 1998, Nature, 394, 344

Zdunik, J., Haensel, P., Paczynski, B., Miralda-Escude, J. 1992, ApJ, 384, 129

TAB. 1: Population syntheses parameters

Physical quantity	Distribution	Values	Units
NS period at t_0^{RLO} (*)	Flat	1 \rightarrow 100	sec
NS μ at t_0^{RLO} (*)	Gaussian	$\text{Log} \langle \mu_0 \rangle = 28.50$; $\sigma=0.32$	G cm^3
\dot{m} in RLO phase (#)	Gaussian	$\text{Log} \langle \dot{m} \rangle = -1.00$; $\sigma=0.50$	\dot{M}_{E}
Minimum accreted mass	One-value	0.01	M_{\odot}
RLO accretion phase time (†)	Flat in Log	$10^6 \rightarrow \tau_{\text{RLO}}^{\text{max}}$ (‡)	year
MSP phase time	Flat in Log	$10^8 \rightarrow 3 \times 10^9$	year

(*) t_0^{RLO} = initial time of the Roche Lobe Overflow phase

(#) baryonic accretion rate during the Roche Lobe Overflow phase

(†) a Maximum accreted Mass of $0.5M_{\odot}$ is permitted during the Roche Lobe Overflow phase

(‡) maximum duration of the Roche Lobe Overflow phase; typical explored values: 5×10^7 yr - 10^8 yr - 5×10^8 yr

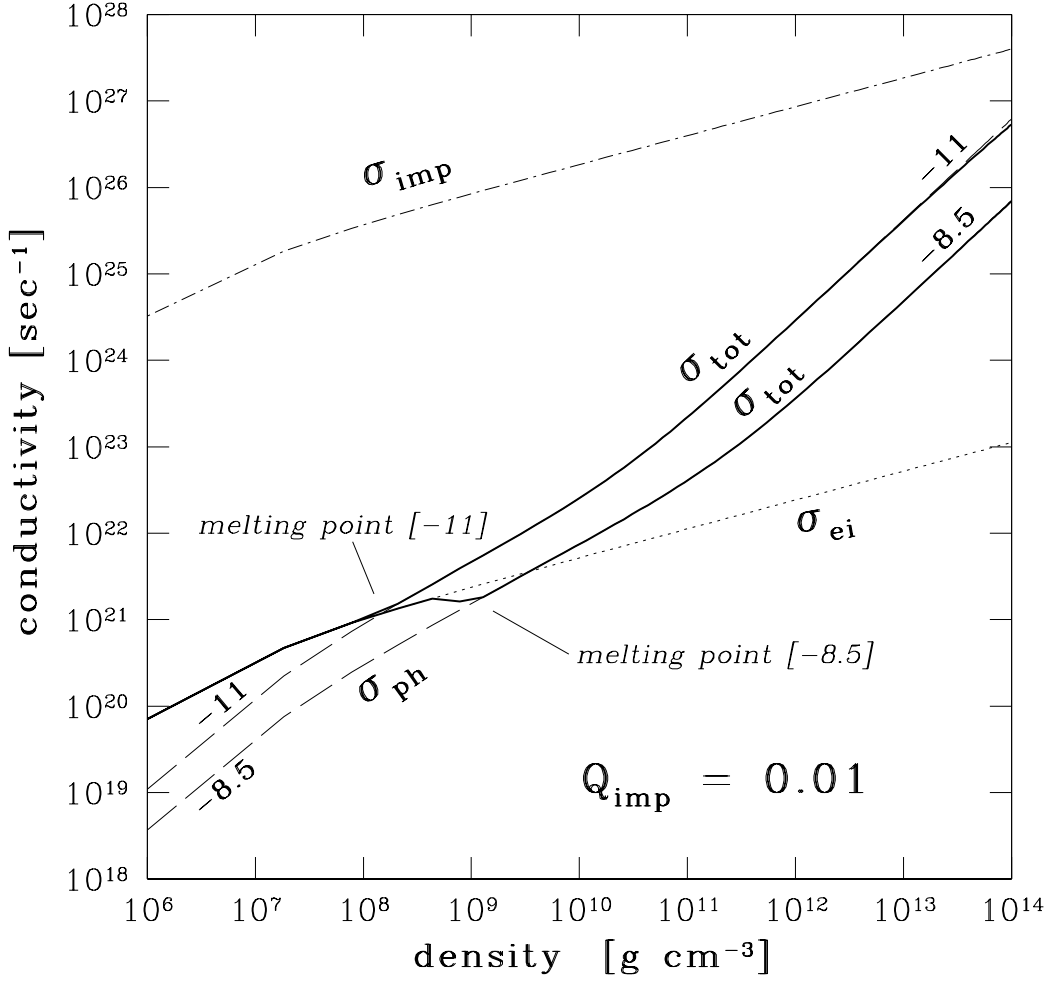


Fig. 1.— The electric conductivity in the crust as a function of the density for $\log(\dot{M}/M_{\odot} \text{yr}^{-1}) = -8.5$ and -11 . The *heavy solid lines* correspond to the total conductivity σ_{tot} . Since the impurity conductivity (σ_{imp} , *dot-dashed line*) is not dependent on the temperature, it is the same for both accretion rates. The conductivity in the liquid region (σ_{ei} , *dotted line*) is determined by electron–ion collisions and also practically not dependent on T , contrary to the phonon conductivity (σ_{ph} , *dashed lines*), which dominates σ_{tot} at highest densities. The shift of the melting point towards higher densities for higher accretion rates is seen.

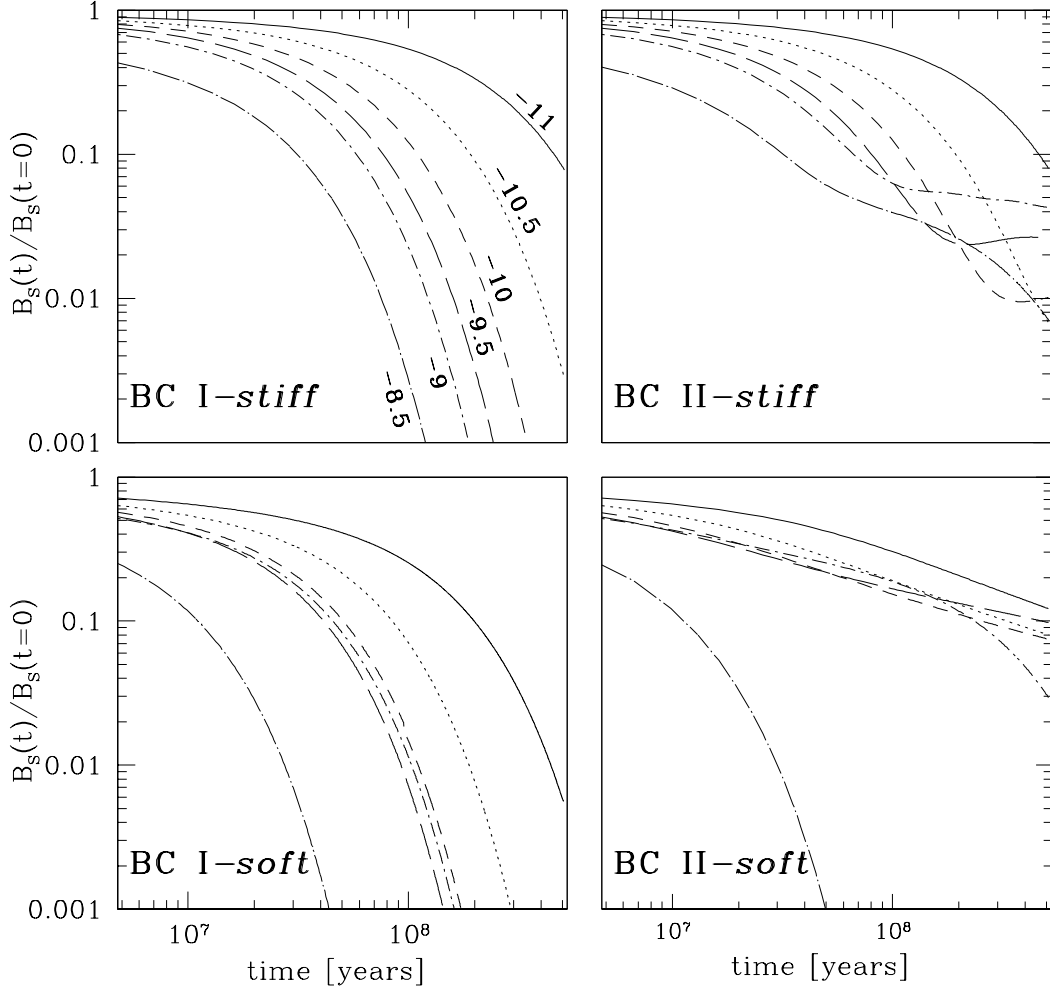


Fig. 2.— The dependence of the surface magnetic field, $B_s(t)$, on the time, normalized on the surface magnetic field strength at the beginning of the RLO phase ($t = 0$). The different accretion rates are labelled according to $\log(\dot{M}/M_\odot \text{ yr}^{-1})$. The four explored cases are located here as in all the following figures: stiff-EoS on the upper panels, soft-EoS on the lower ones; boundary condition BC I on the left panels and BC II on the right.

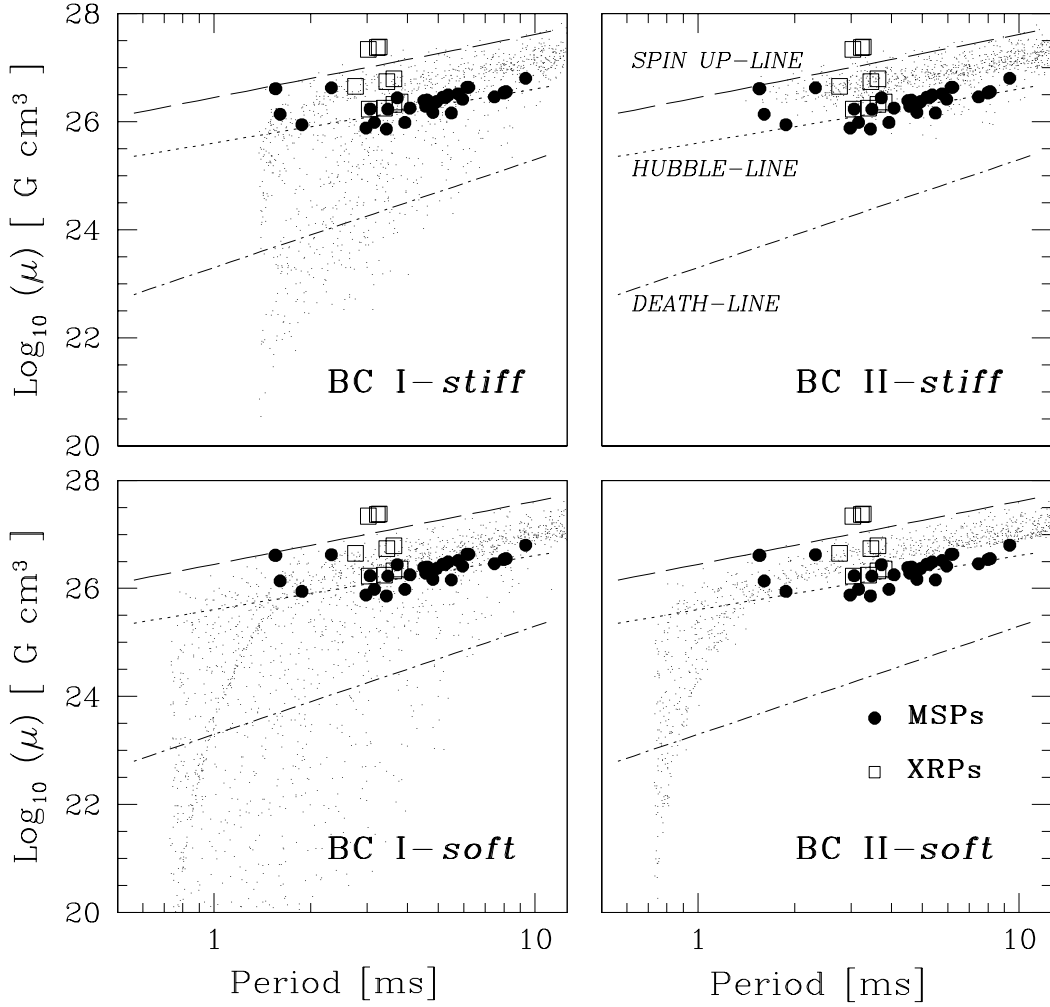


Fig. 3.— Statistical properties of the synthesized populations in the $\mu - P$ plane, for $\langle \dot{m} \rangle = 0.1$ and $\tau_{RLO}^{max} = 5 \times 10^8$ yr. *Full dots* represent the sample of detected MSPs (online catalogue), while *open squares* represent the NSs in LMBs for which the period and the magnetic field have been inferred either from the kHzQPOs seen in their X-ray power spectrum, or from coherent pulsations during burst, as reported in White & Zhang (1997).

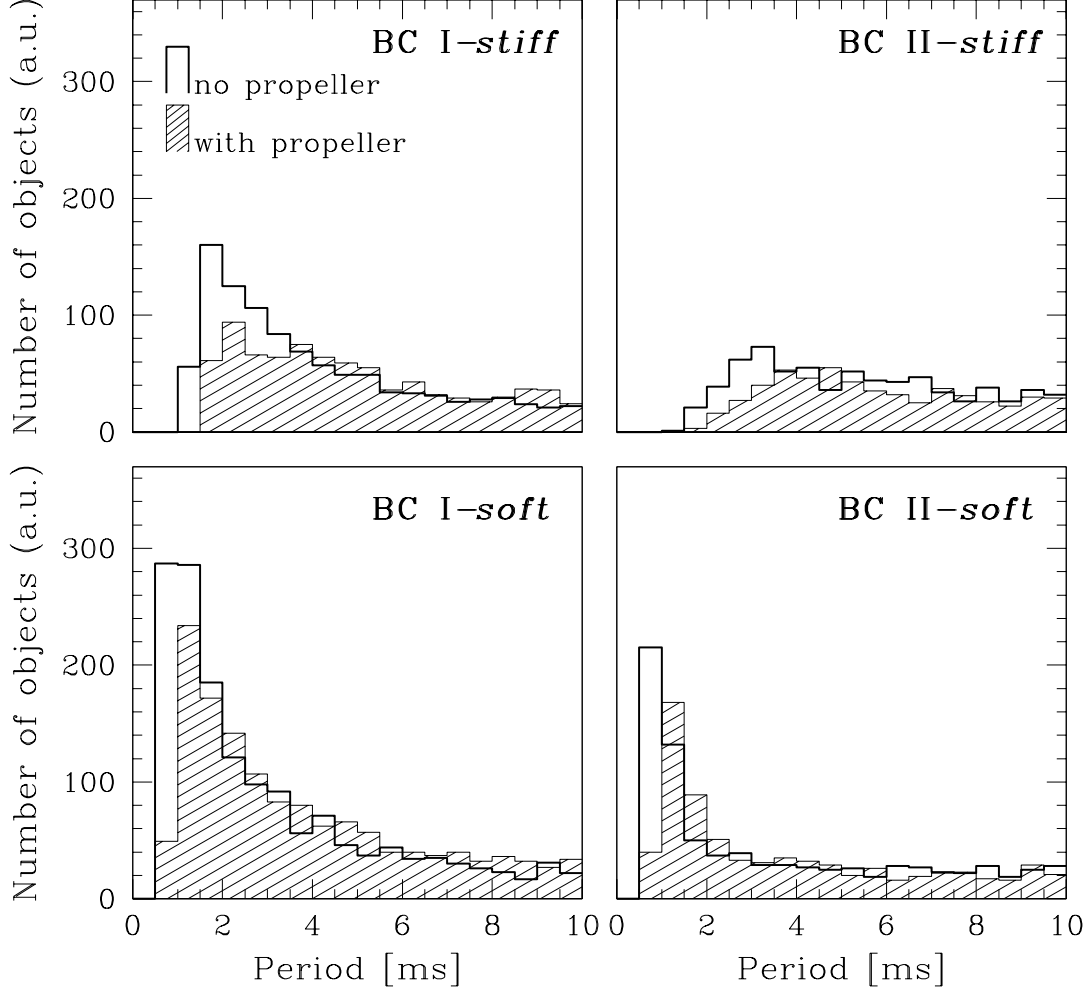


Fig. 4.— Calculated distribution of millisecond NSs as a function of the spin period P . The selected interval is $P_{sh} < P < 10$ ms and μ is let vary over the whole range. *Solid line* denotes the distribution in absence of propeller, whilst *dashed area* give the one with a strong propeller effect included ($\mathcal{F}_{que} = 0.50$ and $\Gamma_{que} = 8$). The absolute number of objects is in arbitrary units.

		BC I		BC II		
<i>stiff</i>	2%	60%	1%	99%		$10^{25.8} \text{ Gcm}^3$
	6%	32%	0%	0%		
<i>soft</i>	4%	42%	11%	57%		$10^{25.8} \text{ Gcm}^3$
	34%	20%	32%	0%		
		1.558 ms		1.558 ms		
standard evolution						

Fig. 5.— Distributions of the synthesized NSs, derived normalizing the sample to the total number of stars with $P < 10$ ms. We have divided the $\mu - P$ plane in four regions. As a guideline the upper left number in each cross gives the percentage of objects having $P < P_{min}$ and $\mu > \mu_{min}$ (the typical variance is about 1%). On the left side, we have indicated the EoS used. The crosses in the first column refer to the boundary condition BC I, whereas those in the second column to BC II.

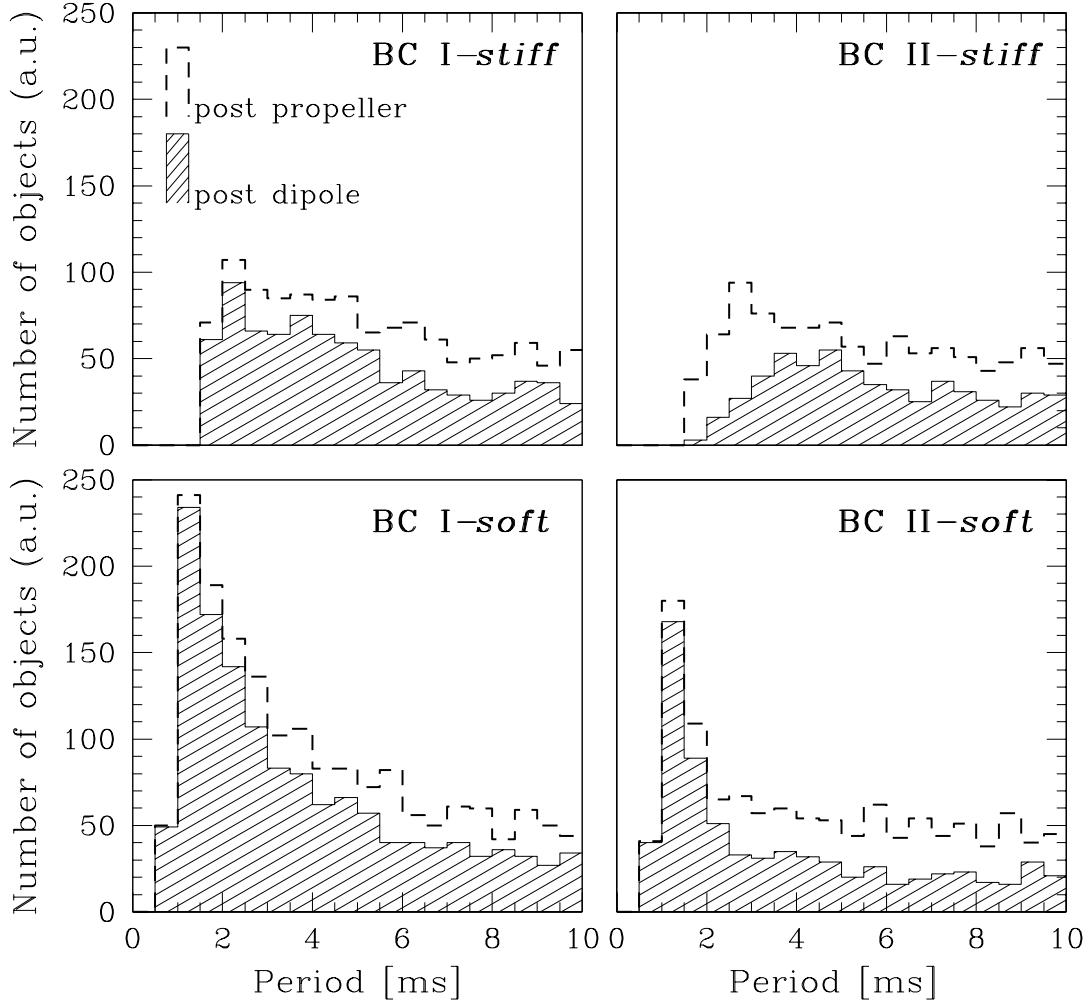


Fig. 6.— The four panels depict the NSs distributions at the end of the propeller phase (dashed lines), and at the end of the magnetic dipole phase (dashed area). μ is kept constant during the radio phase. The propeller is mimicked as for the case of Fig. 4.

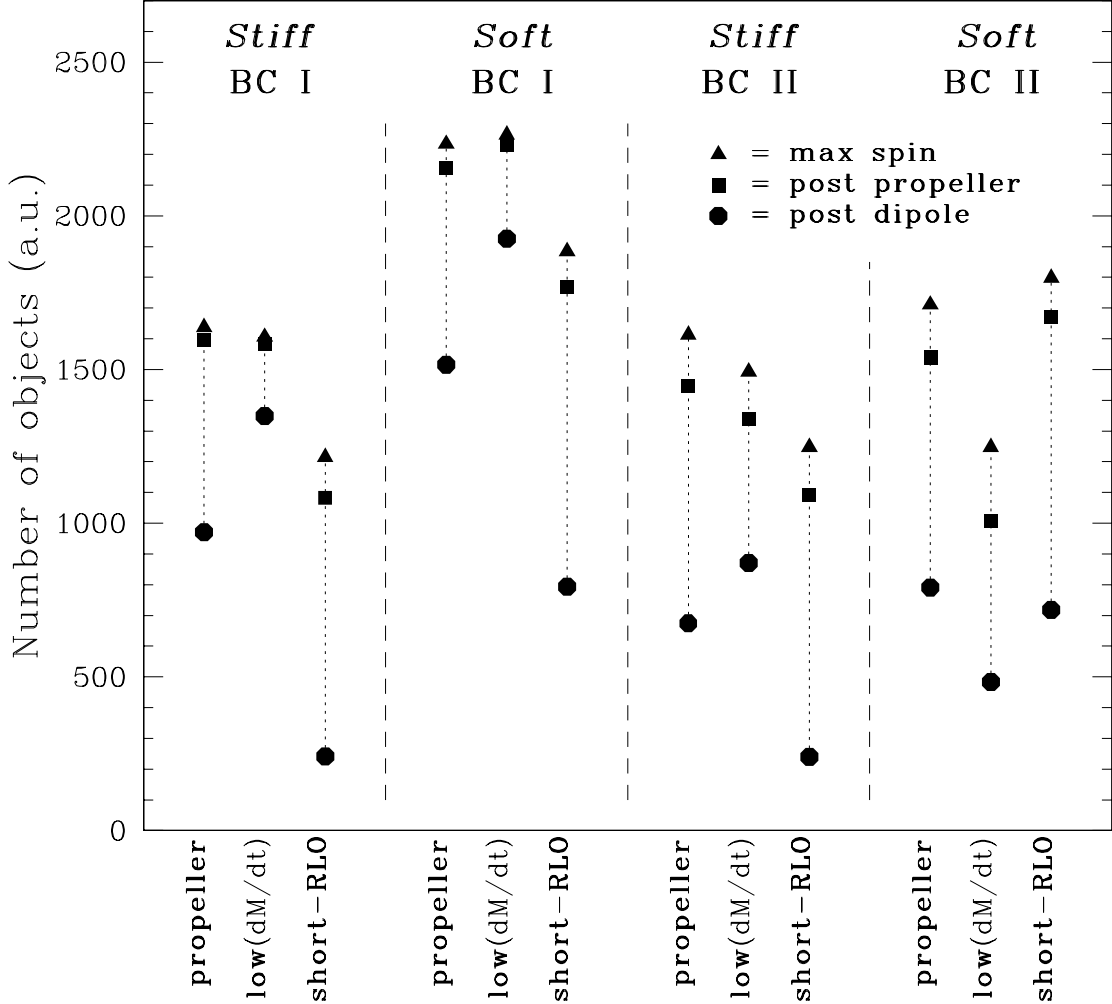


Fig. 7.— Number of synthesized objects with $P < 10$ ms at different stages of their evolution and for different models as indicated in the labels. “Propeller” model refers to $\tau_{RLO}^{max} = 5 \times 10^8$ yr, $\langle \dot{m} \rangle = 0.1$ in Eddington units, $\mathcal{F}_{que} = 0.25$, $\Gamma_{que} = 1$. For the “Low(dM/dt)” model we used $\langle \dot{m} \rangle = 0.01$; while for the “short-RLO” model we adopted $\tau_{RLO}^{max} = 5 \times 10^7$ yr. *Triangles* give the number of NSs at the end of the spinup phase during the RLO; *squares* give the number of NSs at the end of the propeller phase; *big dots* give the number of NSs at the end of the radio phase. The numbers calculated for each models are connected by a thin dotted line. These numbers are in arbitrary units, but with the same normalization for all the cases.

		BC I		BC II			
<i>stiff</i>		0%	54%		0%	100%	$10^{25.8} \text{ Gcm}^3$
		0%	46%		0%	0%	
<i>soft</i>		1%	39%		3%	61%	$10^{25.8} \text{ Gcm}^3$
		21%	39%		28%	8%	
		1.558 ms		1.558 ms			
strong propeller							

Fig. 8.— Distributions of the synthesized NSs, when a strong propeller ($\mathcal{F}_{que} = 0.50; \Gamma_{que} = 8$) is applied. Labels as in Figure 5.

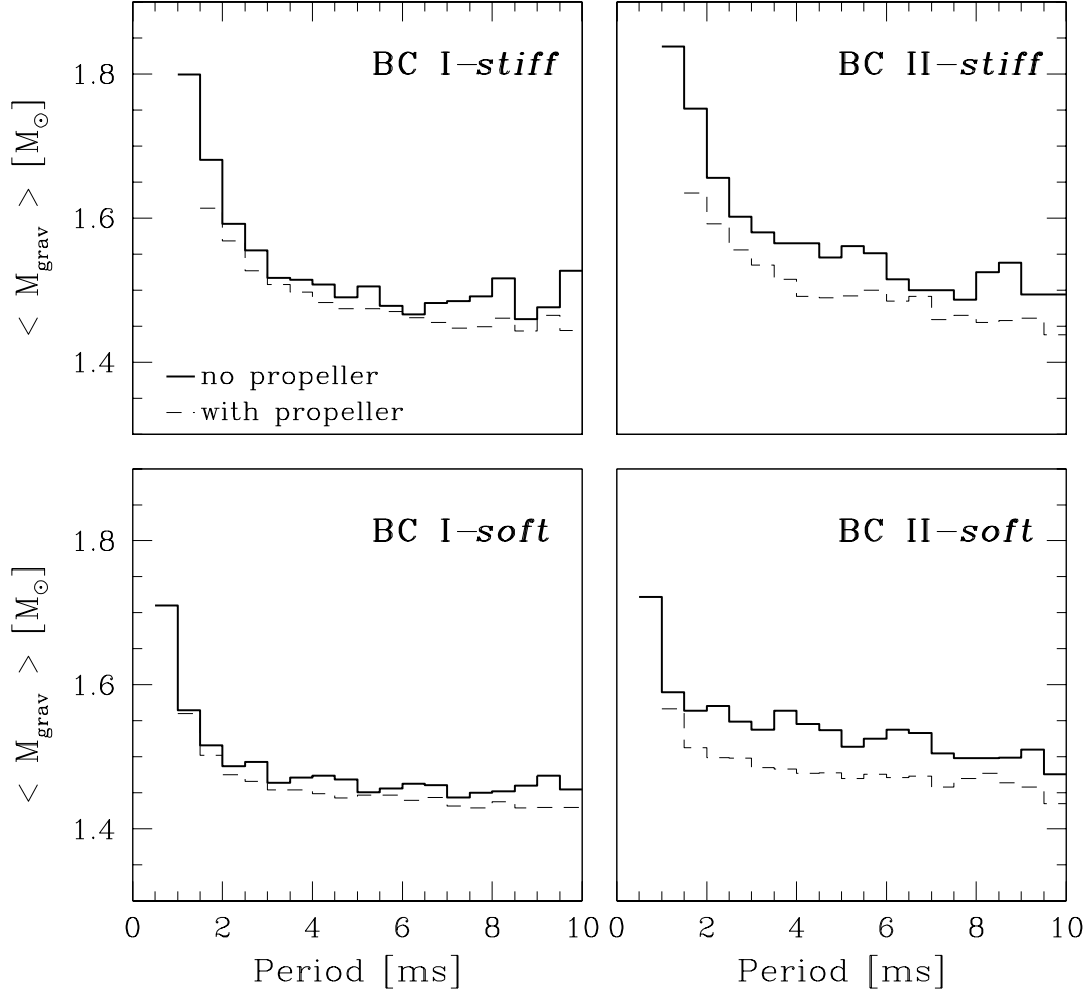


Fig. 9.— Average gravitational masses of the re-accelerated NSs as a function of their final spin period P . μ is let vary over the whole range and the synthesized NSs are binned in 0.5 ms wide intervals. The initial mass of the static NSs is set equal to $1.40M_{\odot}$ for all the cases. *Thick solid line* denotes the mass-distribution in absence of propeller, whereas *thin dashed line* gives the one with a strong propeller effect included ($\mathcal{F}_{que} = 0.50$ and $\Gamma_{que} = 8$).

TAB. 2: Population Syntheses Results

<i>EoS</i>	BC I				BC II				<i>Kind of Evolution</i>	<i>Idx</i>
	<i>Number</i>	<i>Percentage Ratio</i>			<i>Number</i>	<i>Percentage Ratio</i>				
	I	II/I	(II+III)/I	(III+IV)/I	I	II/I	(II+III)/I	(III+IV)/I		
<i>Stiff</i>	689	4.0	14.2 (11.5)	63.5	823	0.3	0.3 (0.3)	0.0	standard	i
	671	1.5	8.6 (6.9)	65.3	774	0.1	0.3 (0.3)	0.0	propeller	ii
	738	0.0	8.4 (2.3)	110.3	1000	0.1	0.3 (0.3)	0.0	low \dot{m} +propeller	iii
	277	0.0	0.0	0.0	275	0.0	0.0	0.0	short _{RLO} +propeller	iv
	125	0.0	0.0	0.0	116	0.0	0.0	0.0	short _{RLO} +low \dot{m} +propeller	v
<i>Soft</i>	742	10.1	91.9 (46.0)	129.0	547	19.4	74.3 (57.3)	54.9	standard	vi
	730	8.0	83.9 (40.5)	131.1	523	16.3	73.8 (55.9)	57.5	propeller	vii
	720	0.6	85.1 (21.1)	207.4	390	12.1	42.5 (34.2)	30.4	low \dot{m} +propeller	viii
	677	17.7	34.2 (34.2)	17.2	640	18.2	28.8 (28.8)	10.6	short _{RLO} +propeller	ix
	410	3.4	7.6 (7.6)	5.9	231	7.0	11.9 (11.9)	5.5	short _{RLO} +low \dot{m} +propeller	x

I = Number of synthesized objects in the first quadrant ($P > P_{min}$ and $\mu > \mu_{min}$). These numbers are normalized to the case (iii) for Boundary Condition BC II, set equal to 1000.

II/I = Percentage ratio of the objects filling the II quadrant over those filling the I quadrant.

(II+III)/I = Percentage ratio of the objects filling the II and the III quadrant over those filling the I quadrant. In parenthesis the percentage ratio of the objects having $P < P_{min}$ and μ above the death line over those filling the first quadrant.

(III+IV)/I = Percentage ratio of the objects filling the III and the IV quadrant over those filling the I quadrant.

Idx = Index for the specific synthesized population. The different kinds of evolution are labelled as in the text.